 doi:10.20944/preprints201806.0047.v1

Title

Artificial membrane induced by novel biodegradable nanofibrous scaffold in the Masquelet procedure for the treatment of segmental bone defects

Authors

Yi-Hsun Yu, M.D.
Department of Orthopedic Surgery, Musculoskeletal Research Center, Chang Gung Memorial Hospital-Linkou, Taoyuan, Taiwan
Department of Mechanical Engineering, Chang Gung University, Taoyuan, Taiwan
Email: alanyu1007@gmail.com
Ren-Chin Wu, M.D.
Department of Pathology, Chang Gung Memorial Hospital-Linkou, Tao-Yuan, Taiwan
Email: renchin.wu@gmail.com
Demei Lee, Ph.D.
Department of Pathology, Chang Gung Memorial Hospital-Linkou, Tao-Yuan, Taiwan
Email: dmlee@mail.cgu.edu.tw
Che-Kang Chen, M.S.
Department of Pathology, Chang Gung Memorial Hospital-Linkou, Tao-Yuan, Taiwan
Email: kevinchenemail@gmail.com
Shih-Jung Liu, Ph.D.
Department of Orthopedic Surgery, Chang Gung Memorial Hospital-Linkou, Taoyuan, Taiwan
Department of Mechanical Engineering, Chang Gung University, Taoyuan, Taiwan
Email: shihjung@mail.cgu.edu.tw

*YH Yu and RC Wu have equal contribution to this study and are co-first authors of this paper.

Correspondence Author: Prof. Shih-Jung Liu, Ph.D.
Biomaterials Lab, Mechanical Engineering
Chang Gung University
259, Wen-Hwa 1st Road
Kwei-Shan, Tao-Yuan 333
Taiwan
Tel: +886-3-2118166, Fax: +886-3-2118558
Email: shihjung@mail.cgu.edu.tw

 doi:10.20944/preprints201806.0047.v1

Abstract

Masquelet induced-membrane technique for the treatment of segmental bone defects includes a two-stage surgical procedure, and polymethylmethacrylate (PMMA) plays a major role in the treatment. However, the PMMA spacer must be surgically removed. Here, we investigated the potential of poly (lactic-co-glycolic acid) (PLGA) nanofibers, a biodegradable material to replace PMMA spacer, allowing the bioactive membrane to be induced, and the spacer to degrade without the additional surgery on a rabbit femoral segmental bone defect model. PLGA nanofibers were shown to degrade completely six weeks after implantation in the investigated animals, and a thick membrane was found to circumferentially fold around the segmental bone defects. Results from image studies demonstrated that, in the group without bone graft, all studied femurs exhibited either nonunion or considerable malunion. In contrast, the femurs in the bone graft group had a high union rate without considerable deformities. Histological examinations suggested that the membranous tissue in this group was rich in small blood vessels and the expression of BMP2 and VEGF increased. Our results demonstrate that the biodegradable PLGA nanofibers may be useful for replacing the PMMA spacer as the bioactive-membrane inducer, facilitating the process of healing and removing the need for repeated surgeries.

Keywords: Biodegradable nanofibers; PLGA; Masquelet technique

Preprints (www.preprints.org) | NOT PEER-REVIEWED | Posted: 5 June 2018 doi:10.20944/preprints201806.0047.v1

1. Introduction

Segmental bone defects may be a result of trauma, tumor resection, or the sequelae of osteomyelitis, and their management remains challenging for orthopedic surgeons [1,2]. Additionally, the development of these defects is accompanied by considerable functional disabilities in patients. Two approaches have been commonly employed for the treatment of segmental bone defects. First, the transplantation of vascularized autologous bone graft [2-4] has been commonly used, however, the donor site morbidity from the autologous fibula graft, including infection and stress fracture, remains as the main concern. In addition, the operation must be performed by a microsurgery specialist [4]. The second approach is the bone transport with distraction osteogenesis by Ilizarov ring fixator, which is a standard procedure for the management of segmental bone defect applied by the experienced surgeons in some medical institutes [5-7]. Nevertheless, various complications, including pin tract infection, failure of the transported bone consolidation, and nonunion at the docking site have been reported [8,9].

An alternative approach for the segmental bone defect repair was first proposed by Masquelet in 1980 [10], showing that, following the implantation of a polymethylmethacrylate (PMMA) spacer for 6 to 8 weeks in the segmental cortical bone defect, a periosteum-like membrane surrounding the defect,

Preprints (www.preprints.org) | NOT PEER-REVIEWED | Posted: 5 June 2018 doi:10.20944/preprints201806.0047.v1

containing osteogenic and osteoinductive factors, can be induced. This PMMA-induced bioactive membrane serves as an envelope, encapsulating the autologous cancellous bone graft and promoting bone healing. Other studies, following this two-stage Masquelet procedure, demonstrated satisfactory results for bone union [11-17]. In spite of the promising outcomes achieved using this technique, one major drawback pertains to be the requirement for the surgical removal of the PMMA spacer, demanding the patients to undergo several surgeries and thus increasing the cost and complexity of the treatment.

Since the actual mechanisms underlying the formation of induced membrane have not been completely elucidated, we aimed to examine whether the PMMA spacer can be replaced by a different biodegradable implant, in order to avoid the requirement for an additional surgical intervention during the Masquelet procedure. Therefore, we developed biodegradable nanofibrous implants and examined their ability to induce bioactive membranes using the segmental bone defect model. Additionally, we investigated the role of biodegradable implants as the reservoirs for bone grafting during the formation of the bioactive membrane, which facilitates fracture healing.

Preprints (www.preprints.org) | NOT PEER-REVIEWED | Posted: 5 June 2018 doi:10.20944/preprints201806.0047.v1

2. Materials and methods

Preparation of poly (lactic-co-glycolic acid) (PLGA) nanofibers

PLGA polymers (LA:GA=50:50, Sigma, USA) were adopted. An electrospinning setup was employed to produce the nanofibers. A high-voltage of 17 kV was applied to the needle that emits the solution jet. The distance of the needle to the collecting plate and the flow rate of the syringe were 12 cm and 0.5 mL/h, respectively. Fabricated nanofibrous membrane was incubated in a chamber equipped with a vacuum pump at 40°C for three days to volatilize the solvent.

Scanning electron microscope (SEM) characterization

The morphological structure of the polymeric fibers was characterized by a JEOL Model JSM-7500 F field emission SEM (Tokyo, Japan).

In vivo study and animal care

This study and all procedures used acquired approval from the Institutional Review Board and Animal Care Center of Chang Gung University, Taiwan (IRB number: CGU106-058). Twelve 6-month-old male New Zealand rabbits were cared and grown using the standardized procedures of the Animal Care Center of Chang Gung University. Rabbits were housed in individual pens with free access to food and water. All the studied rabbits had comparable weights (3.0

Preprints (www.preprints.org) | NOT PEER-REVIEWED | Posted: 5 June 2018 doi:10.20944/preprints201806.0047.v1

±0.2 kg).

Prior to the surgeries, oxygen was delivered to the animals via a face mask at a flow rate of at 4 L/min for five minutes. Isoflurane was then transmitted via the face mask till the rabbit became anesthetized and continued during the entire surgical procedure. Rabbits were kept in the decubitus position which allowed the surgical field upwards, and the right thighs were shaved and disinfected. A longitudinal incision was made along the lateral aspect of the thigh, and an internervous plane was created bluntly between the vastus lateralis and biceps femoris to expose antero-lateral aspect of the femur (Figure 1a). Afterward, the femur was fixed with a 10-hole stainless-steel plate (Lisen Technology Co. Ltd., New Taipei City, Taiwan) with two 2.0-mm screws at each end, and 1.8-mm Kirschner wire was inserted intramedullary from intercondylar notch of the femur retrogradely. After stabilization, a critical-size bone defect, measuring 10 mm, was created in the middle of femur shaft using an osteotome (Figure 1b).

Following the creation of the defect, the defect was wrapped circumferentially with the PLGA nanofibers (Figure 1c), and we randomized the operated rabbits into two groups: bone graft-free (BG-f) and bone graft (BG) groups. In the BG-f group, the nanofibers were sutured at the both ends with 3-

Preprints (www.preprints.org) | NOT PEER-REVIEWED | Posted: 5 June 2018 doi:10.20944/preprints201806.0047.v1

0 Vicryl (Ethicon, Johnson & Johnson, New Jersey, USA) suture to secure the wrapping, leaving the inside of the wrapped nanofiber empty (Figure 1d), while in the BG group, the same wrapping procedure was completed after placing the bone chips, obtained from the osteotomized femur by chipping of the cortical bone, inside the wrapped PLGA nanofibers (Figure 1e).

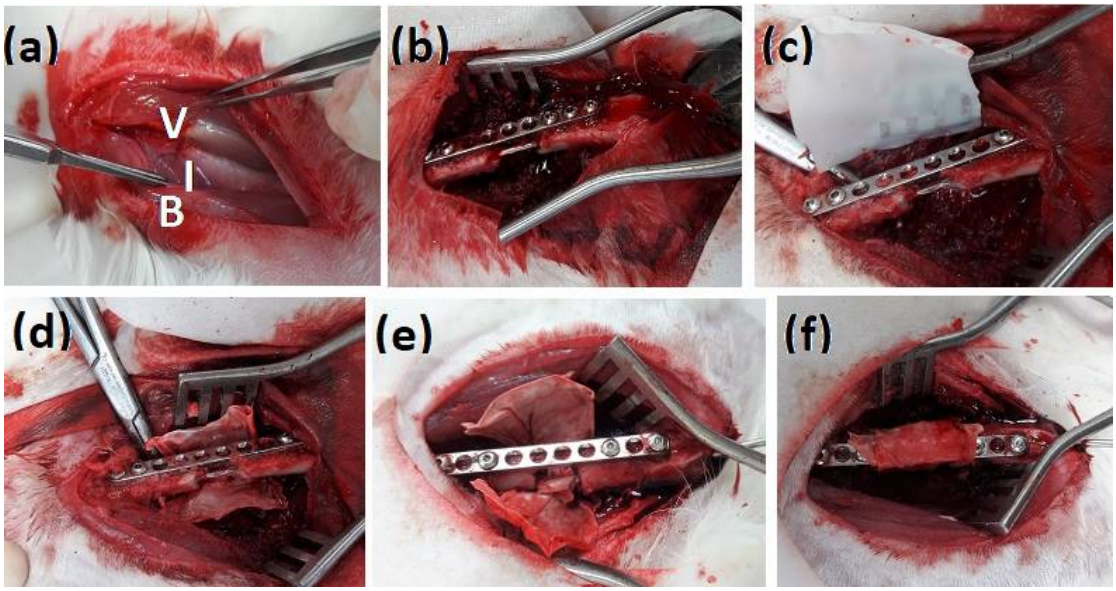

Figure 1 Surgical procedure applied for the formation and treatment of the segmental bone defect in a rabbit model. (a) Identification the internervous plane (I) between the vastus lateralis (V) and biceps femoris (B). (b) Creation of a 10-mm femoral defect following the fixation procedure with stainless plate and intramedullary nail. (c) Application of PLGA nanofibers around the bone defect. (d) Suture-fixation of the PLGA nanofibers in BG-f group. (e) Bone grafting (BG) inside the femoral defect before the suture-fixation of the PLGA nanofibers.

Preprints (www.preprints.org) | NOT PEER-REVIEWED | Posted: 5 June 2018 doi:10.20944/preprints201806.0047.v1

Afterward, the wound was irrigated with sterile saline and the fascia of vastus lateralis and biceps femoris were approximated using 2-0 Vicryl suture, while the subcutaneous tissue and skin were occluded using 3-0 Vicryl suture (Ethicon, Johnson & Johnson, New Jersey, USA).

All animals were monitored daily for any altered behavior or complications, and analgesics were administered for 5 days postoperatively. They were allowed free movements and full weight bearing immediately following the recovery from anesthesia. The rabbits were also checked twice daily for mentation and attitude, ability to ambulate, willingness to bear weight on the surgically treated limb, food and water consumption, respiratory rate, and inflammation at the surgical site.

All the rabbits were euthanized 6 weeks after the surgical procedure by a standard euthanasia procedure. The entire femur was harvested through the plane used in the previous surgical procedures. Periosteal and fibrous tissues surrounding the defects were preserved. The observed membranes were excised carefully and further analyzed. Femur samples were fixed in 10% neutral buffered formalin for 48 h and transferred to 70% ethanol, until further X-ray and micro-computed tomography (CT) studies.

Preprints (www.preprints.org) | NOT PEER-REVIEWED | Posted: 5 June 2018 doi:10.20944/preprints201806.0047.v1

X-ray and micro-CT examinations

The animals underwent X-ray examinations twice: immediately after the surgical procedure and after euthanasia at six weeks. Prior to the first radiative inspection, the animals were consoled with an intravenous injection of zolazepam/tiletamine (Zoletil, Taipei, Taiwan). X-ray images of the anteroposterior and lateral views were obtained. During the second X-ray imaging, the target femora were evaluated using micro-CT as well.

Histologic analysis

Capsular tissue processing

Capsular tissue samples obtained from the investigated animals were preserved in 10% phosphate-buffered formalin and sliced into 2-mm wide fragments, which were processed and embedded in paraffin. Tissue sections (4 μm) were obtained using a microtome (Sakura Finetek, Tokyo, Japan) for histological and immunohistochemical (IHC) evaluations. Additionally, the obtained samples were blotted with H&E and observed under a microscope with magnification up to 400×.

IHC staining of capsular tissue

IHC staining was performed on 4-μm tissue sections using an automated

Preprints (www.preprints.org) | NOT PEER-REVIEWED | Posted: 5 June 2018 doi:10.20944/preprints201806.0047.v1

stainer (BOND-MAX, Leica Microsystems, Singapore). After deparaffinization, heat-induced epitope retrieval was performed (100°C/20 min) in EDTA buffer (pH 9). For bone morphogenic protein (BMP2) analysis, a mouse anti-BMP2 monoclonal antibody (1:200; clone 65529.111, Cat# ab6285, Abcam, Cambridge, UK) was adopted as the primary antibody. For the characterization of vascular endothelial growth factor (VEGF), a mouse anti-VEGF antibody (1:400; clone VG1, Cat#: NB100-664, Novus Biologicals, Littleton CO, USA) was used. PolyTek goat anti-mouse polymerized horseradish peroxidase (HRP; Scytek Laboratories, Logan, UT, USA) was employed as the secondary antibody. Bond Polymer Refine Detection Kit (DS9800, Leica Microsystems, Singapore) was applied for the visualization of obtained signals.

3. Results

SEM analysis PLGA of nanofibers

The microscopic photos of the biodegradable nanofibers are displayed in Figure 2 (x8,000). Measured diameters of PLGA nanofibers spanned from 40 to 430 nm.

Preprints (www.preprints.org) | NOT PEER-REVIEWED | Posted: 5 June 2018 doi:10.20944/preprints201806.0047.v1

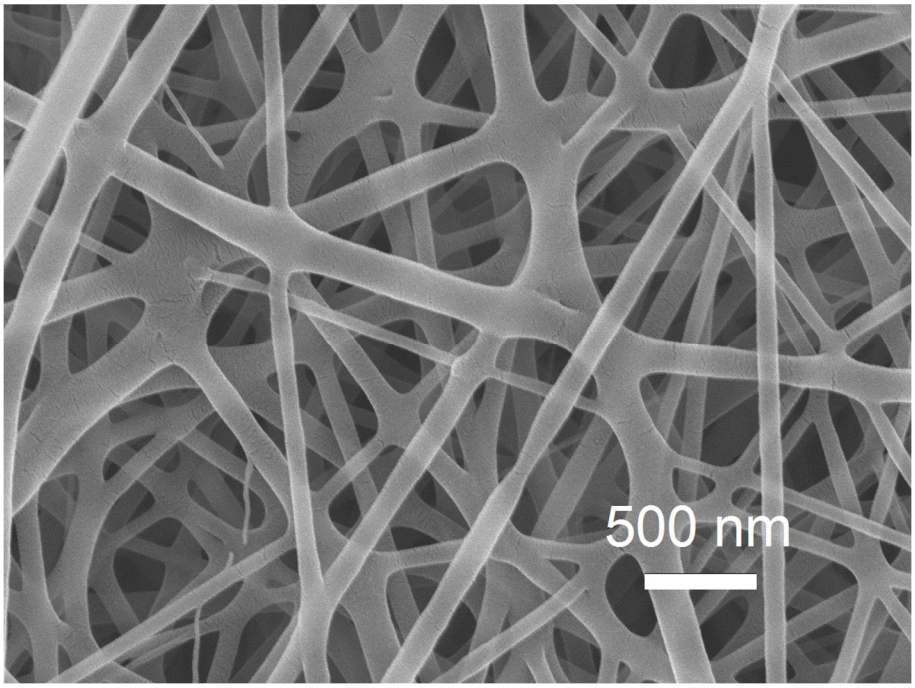

Figure 2 The SEM photographs of fabricated nanofibers.

Femoral sample examination

After euthanizing the rabbits and excising the target femora, we observed that in all specimens, a membranous layer was observed to surround the applied PLGA nanofibers densely, immediately between the applied material and the muscles (Figure 3).

Preprints (www.preprints.org) | NOT PEER-REVIEWED | Posted: 5 June 2018 doi:10.20944/preprints201806.0047.v1

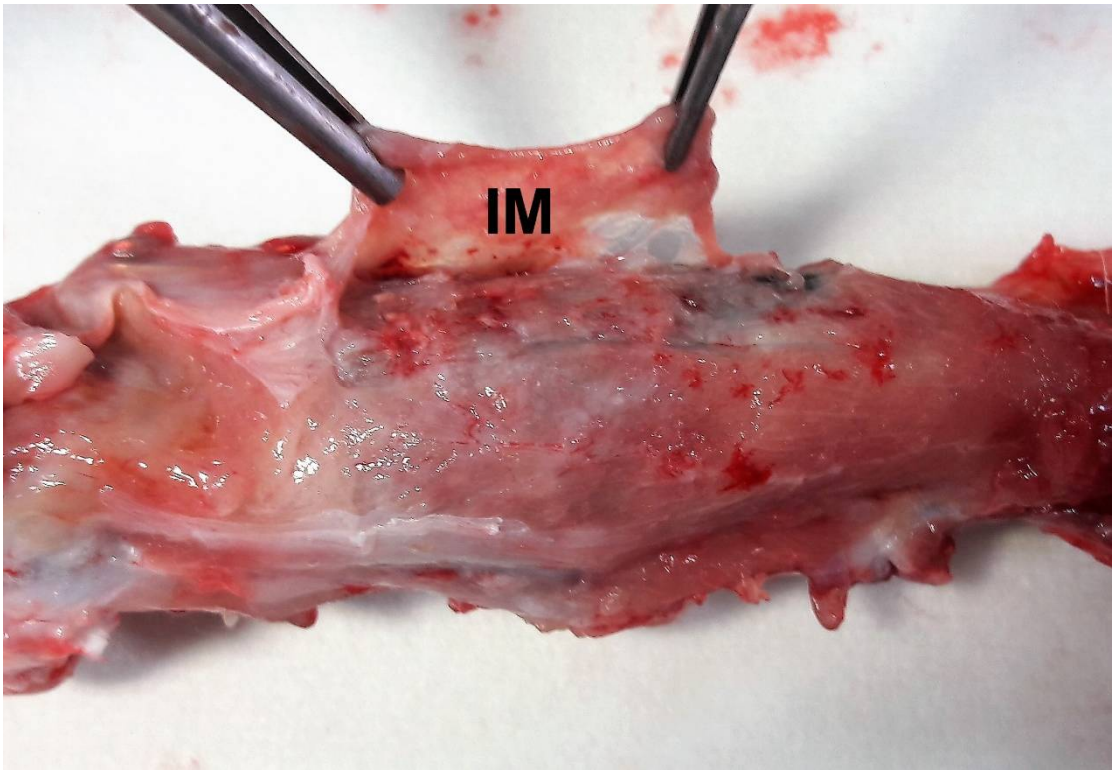

Figure 3 Induced membrane formation. Identification of the induced membrane (IM) around the poly (lactic-co-glycolic acid) nanofibers in a representative rabbit femoral specimen.

In the BG group, the femoral samples were shown to have continuous hard calluses without any considerable deformities, shortening of the osteotomized femurs, or loosened implants (Figure 4a). In contrast, in the BG-f group, various adverse effects of the implantation were observed, such as residual fracture gap in the calluses, loosened screws, changes in the position of the intramedullary K wires, and considerable malunion rate and the shortening of the femur (Figure 4b).

Preprints (www.preprints.org) | NOT PEER-REVIEWED | Posted: 5 June 2018 doi:10.20944/preprints201806.0047.v1

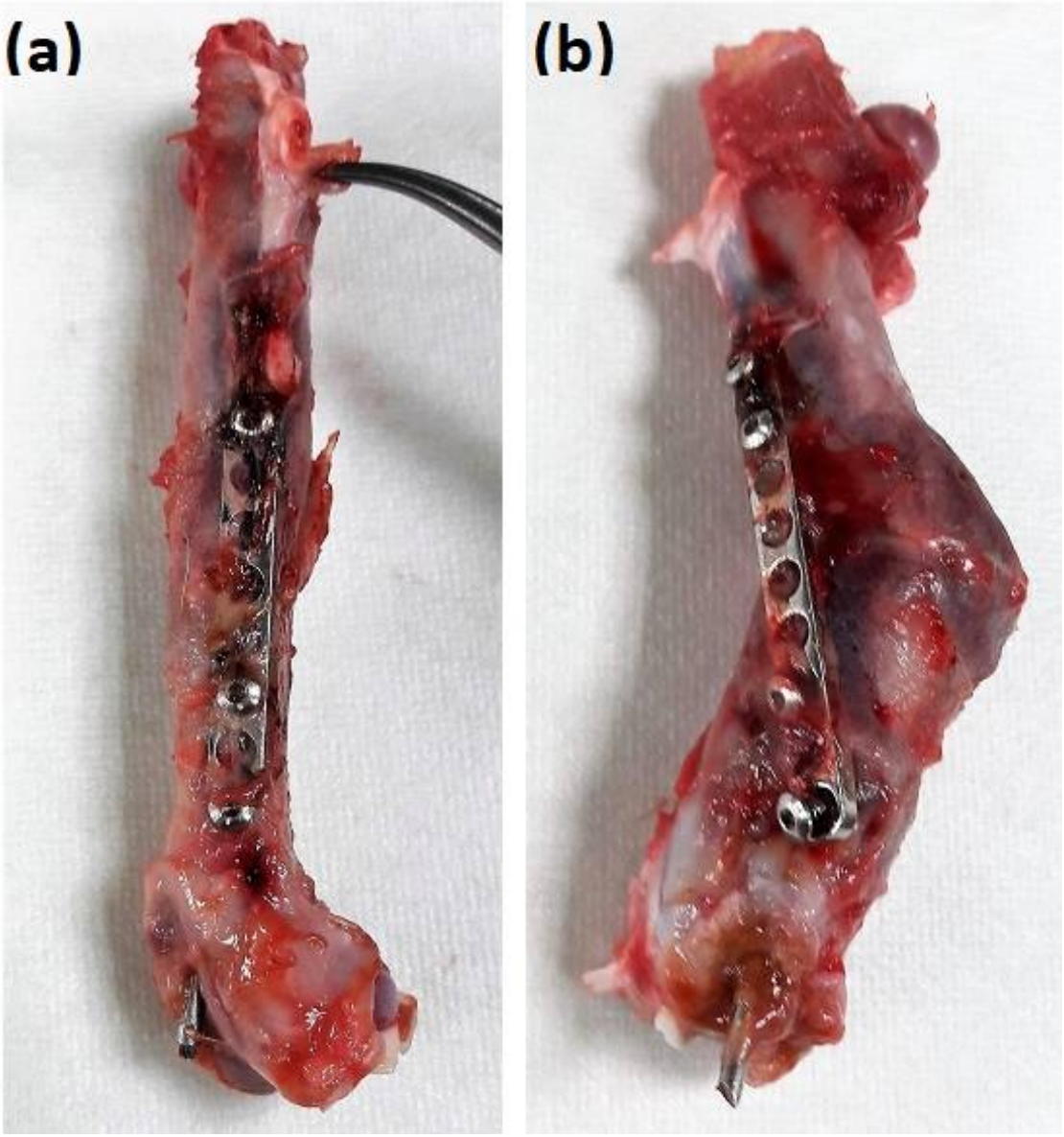

Figure 4 Representative images of the examined femoral defects after the rabbit euthanization. (a) Representative images of the BG group femur, showing a continuous femoral cortex with good union rate without deformity. (b) Representative images of a malunited femur obtained from an animal included in the BG-f group, with the loss of the fixation of applied fixators.

Preprints (www.preprints.org) | NOT PEER-REVIEWED | Posted: 5 June 2018 doi:10.20944/preprints201806.0047.v1

X-ray and micro-CT results

As observed in the follow-up series of X-ray images obtained in the BG-f group, four femurs failed to achieve bone union, leading to the residual bony gaps, while two femurs were malunited with considerably deformity and shortening rates (Figure 5a). In contrast, in the BG group, only one femoral sample was shown to have a residual gap on one side. Five tissue samples were found to achieve bone union without serious deformities (Figure 5b), while one sample had a loosed implant with some degree of shortening and malunion. Micro-CT examinations revealed united bone gaps and good bone remodeling in the BG group (Figure 5C), with good callus formation and continuous femoral cortex.

Figure 5 X-ray and micro-computed tomography (CT) evaluations of the treated femoral defects. (a) Representative X-ray images of the treated femoral defects

Preprints (www.preprints.org) | NOT PEER-REVIEWED | Posted: 5 June 2018 doi:10.20944/preprints201806.0047.v1

in the BG-f group. (b) Representative X-ray images of the treated femoral defects in the BG group. R, a residual gap in one femur belonging to this group. (c) Representative micro-CT images of the treated femoral defects in the BG group.

Histologic and IHC characteristics of the capsules

The surfaces of the capsular membranes in both groups were found to be lined by one to three layers of round to ovoid cells or short spindle cells (Figure 6a). These cells were shown to lack the underlying basement membrane and morphologically resembled synoviocytes. The deeper layers of the membranes consisted of fibroblast-like spindle cells with longer cytoplasmic processes and haphazard orientation in an extracellular matrix-rich stroma. Membranous tissue was rich in small blood vessels. Scattered eosinophils and lymphocytes were noted in most cases, and multinucleated giant cells were occasionally identified.

IHC staining revealed that the membrane-lining cells and spindle cells showed a diffuse and strong cytoplasmic expression of BMP2 (Figure 6b), with the moderate expression of VEGF, whereas the vascular endothelial cells

Preprints (www.preprints.org) | NOT PEER-REVIEWED | Posted: 5 June 2018 doi:10.20944/preprints201806.0047.v1

exhibited intense cytoplasmic VEGF staining (Figure 6c).

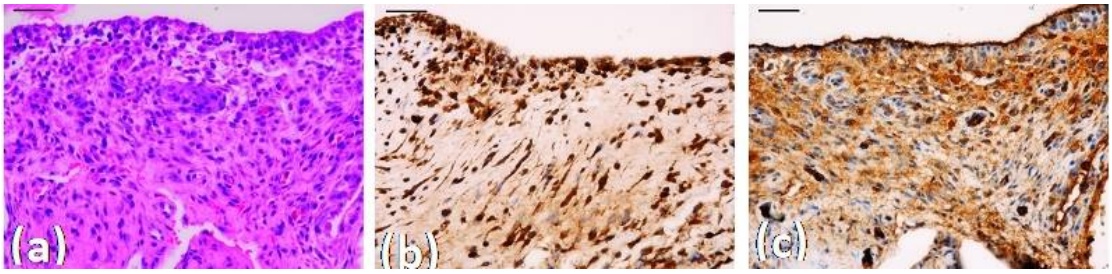

Figure 6 Histologic and immunohistochemical examination of the femoral samples. (a) Capsular membrane stained with hematoxylin and eosin. (b) BMP2 and (c) VEGF expression in the femoral samples. Scale bars, 50 μm.

4. Discussion

In this study, we examined the effectiveness of the PLGA nanofibers used in the Masquelet technique for the induction of periosteum-like bioactive membrane and the reparation of the segmental bone defects. Our results demonstrated that the bioactive membrane can be successfully induced by the application of the biodegradable material tested here, PLGA, which was shown to be accompanied by the expression of growth factors such as BMP2 and VGEF. PLGA nanofibers were shown to play an important role as the bone graft reservoirs, assisting fracture union in the segmental femoral defect model.

Biodegradable materials have been widely employed in medical

Preprints (www.preprints.org) | NOT PEER-REVIEWED | Posted: 5 June 2018 doi:10.20944/preprints201806.0047.v1

procedures since the 1970s. They have been applied in the orthopedic surgeries, as internal fixators [18,19], drug delivery media [20-22], and bone graft reservoirs [23,24]. PLGA has been one of the most prospective biodegradable polymers, mainly due to its controllable degradation and superior biocompatibility with the human tissues. This polymeric material has received approval for clinical applications, owing to that it is innocuous, evokes an acceptable inflammation, and can be degraded via the hydrolysis of its ester bond [25]. These end products may induce inflammatory responses in the surrounding tissue, recruiting fibroblasts, inflammatory cells, and stimulating angiogenesis. Additionally, we supposed that inflammatory responses due to the degradation of the biodegradable materials may induce tissue adhesion, leading to the formation of an encapsulated cavity, which may play a role as a reservoir for bone grafts. We demonstrated here that the PLGA fibers induced the formation of a mature periosteum-like membrane circumferentially wrapped around the fibers. These nanofibers were shown to be hydrolyzed and degraded at the time of examination, while the cells localized in the healing tissue expressed osteoinductive factors such as BMP2 and VGEF.

The Masquelet technique combined with a two-stage external and internal fixation has been widely accepted as a standard in the treatment of

Preprints (www.preprints.org) | NOT PEER-REVIEWED | Posted: 5 June 2018 doi:10.20944/preprints201806.0047.v1

large bone defects: the first stage consists of radical debridement, limb stabilization, PMMA spacer implantation, and soft tissue coverage, while the second stage consists of the clearance of infection, if infective nonunion locations exist, removal of PMMA spacer, massive autologous cancellous bone grafting, and a permanent internal fixation [28-30]. The implantation of the PMMA spacer is a crucial step in this procedure, as it prevents the fibrous tissues from invading the bone defect (mechanical role), and induces the growth of surrounding membrane (biological role) that envelops bone grafts and stimulates bone healing mediated by osteoinductive growth factors [26,27,31]. However, the PMMA cement spacer needs to be surgically removed, so that the bone graft can be implanted within the “envelop” generated by the PMMA spacer. The PLGA nanofibers examined in this study exhibited a similar ability to induce the development of bioactive membranes, as shown by histologic and IHC analyses. Additionally, bone healing process was shown to proceed simultaneously with the degradation of the PLGA nanofibers in the BG group, indicating that these grafts were securely fixed inside the PLGA nanofiber layer. With the formation of the induced membrane and degradation of the PLGA nanofibers, new bone formation was stimulated, suggesting that the PLGA nanofibers and this membrane may play a role of a bone graft reservoir. By

Preprints (www.preprints.org) | NOT PEER-REVIEWED | Posted: 5 June 2018 doi:10.20944/preprints201806.0047.v1

using the biodegradable nanofibers, the original two-stage Masquelet procedure can be reduced to a single step, decreasing the time, cost, and patient discomfort associated with the treatment, in addition to minimizing the risk of surgical site infection.

Our study has several limitations. First, the rabbits used in the study were all euthanized at 6 weeks, and this time point was selected based on the timing of the standard Masquelet procedure, as in previous studies.[12-16] To the best knowledge of the authors, this research was the pioneer one to use biodegradable material to induce bioactive membrane. Therefore, the actual time necessary to induce membrane formation was unknown. However, we successfully induced bioactive membrane formation, which the results of our analyses confirmed. Furthermore, due to the loss of the fixation of one femur in the BG group, it shape was shown to be deformed, with the bone shortening. However, the results obtained from both groups demonstrated that the preservation of bone grafts is crucial for bone healing. Finally, we did not quantify the obtained micro-CT results, failing to determine the quantitative difference between the analyzed groups. However, the union rates can be determined from the photographs and X-ray images. In future, these differences should be quantified.

Preprints (www.preprints.org) | NOT PEER-REVIEWED | Posted: 5 June 2018 doi:10.20944/preprints201806.0047.v1

5. Conclusion

In conclusion, in this study, we successfully used the PLGA nanofibers as a biodegradable material in Masquelet technique, which were shown to induce the generation of bioactive membranes, envelope bone grafts, and enhance bone union. We demonstrated additionally that this material can replace the PMMA in the treatment of large bone defects, and it does not need to be removed. Further studies should focus on the duration of post-operative induction of membrane formation and the use of different biodegradable materials with the better performance than the PLGA nanofibers.

Acknowledgements

The financial supports of the Ministry of Science and Technology, Taiwan (Contract No. 104-2221-E-182-048-MY3) and Chang Gung Memorial Hospital (Contract No. CMRPD2H0031) for this research are gratefully acknowledged.

Author Contributions

Conceptualization: Y.-H.Y. and S.-J.L.; Funding acquisition S.-J.L.; Investigation: Y.-H.Y. and C.-K.C.; Writing: Y.-H.Y. and R.-C.W.; Writing - Review and Editing: D.L.; Supervision S.-J.L.

 doi:10.20944/preprints201806.0047.v1

Conflicts of Interest

The authors declare that there is no conflict of interest

 doi:10.20944/preprints201806.0047.v1

References

1. Hake, M.E.; Oh, J.K.; Kim, J.W.,; Ziran, B.; Smith, W.; Hak, D.; Mauffrey, C. Difficulties and challenges to diagnose and treat posttraumatic long bone osteomyelitis. *Eur J Orthop Surg Traumatol*. 2015, 25(1), 1-3.

2. Nauth, A.; McKee, M.D.; Einhorn, T.A.; Watson, J.T.; Li R.; Schemitsch, E.H. Managing bone defects. *J Orthop Trauma*. 2011, 25(8), 462-466.

3. Taylor, G.I.; Miller, G.D.; Ham, F.J. The free vascularized bone graft. A clinical extension of microvascular techniques. *Plast Reconstr Surg.* 1975, 55(5), 533–544.

4. Molina, C.S.; Stinner, D.J.; Obremskey, W.T. Treatment of traumatic segmental long-bone defects. A critical analysis review. *JBJS Rev.* 2014, 2(4).

5. Madhusudhan, T.R.; Ramesh, B.; Manjunath, K.; Shah H.M.; Sundaresh, D.C.; Krishnappa, N. Outcomes of Ilizarov ring fixation in recalcitrant infected tibial non-unions—a prospective study. *J Trauma Manag Outcomes.* 2008, 2(1), 6.

6. Oh, C.W.; Apivatthakakul, T.; Oh, J.K.; Kim, J.W.; Lee, H.J.; Kyung, H.S.;

Baek, S.G.; Jung, G.H. Bone transport with an external fixator and a locking plate for segmental tibial defects. *Bone Joint J.* 2013, 95-B(12), 1667-1672.

7. Demiralp, B.; Ege, T.; Kose, O.; Yurttas, Y.; Basbozkurt, M. Reconstruction of intercalary bone defects following bone tumor resection with segmental bone transport using an Ilizarov circular external fixator. *J Orthop Sci*. 2014, 19(6), 1004–1011.

8. Chaddha, M. Gulati, D. Singh, A.P.; Singh, A.P. Maini, L. Management of massive posttraumatic bone defects in the lower limb with the Ilizarov technique. *Acta Orthop Belg.* 2010, 76(6), 811–820.

9. Giannoudis, P.V. Treatment of bone defects: bone transport or the induced membrane technique? *Injury.* 2016, 47(2), 291–292.

10. Masquelet, A.C.; Fitoussi, F.; Begue, T.; Muller, G.P. Reconstruction of the long bones by the induced membrane and spongy autograft. *Ann Chir Plast Esthet.* 2000, 45(3), 346–353.

11. Pelissier, P.; Martin, D.; Baudet, J.; Lepreux, S.; Masquelet, A.C. Behaviour of cancellous bone graft placed in induced membranes. *Br J*

Plast Surg. 2002, 55(7), 596–598.

12. Karger, C.; Kishi, T.; Schneider, L.; Fitoussi, F.; Masquelet, A.C.; for French Society of Orthopaedic Surgery and Traumatology (SoFCOT). Treatment of posttraumatic bone defects by the induced membrane technique. *Orthop Traumatol Surg Res*. 2012, 98(1), 97-102.

13. Taylor, B.C.; Hancock, J.; Zitzke, R.; Castaneda, J. Treatment of bone loss with the induced membrane technique: techniques and outcomes. *J Orthop Trauma*. 2015, 29(12), 554-557.

14. Olesen, U.K.; Eckardt, H.; Bosemark, P.; Paulsen, A.W.; Dahl, B.; Hede, A. The Masquelet technique of induced membrane for healing of bone defects. A review of 8 cases. *Injury*. 2015, 46 Suppl 8, S44-S47.

15. Scholz, A.O.; Gehrmann, S.; Glombitza, M.; Kaufmann, R.A.; Bostelmann, R.; Flohe, S.; Windolf, J. Reconstruction of septic diaphyseal bone defects with the induced membrane technique. *Injury*. 2015, 46 Suppl 4, S121-S124.

16. Ronga, M.; Ferraro, S.; Fagetti, A.; Cherubino, M.; Valdatta, L.; Cherubino, P.; Masquelet technique for the treatment of a severe acute tibial bone

loss. *Injury.* 2014, 45 Suppl 6, S111-S115.

17. Morris, R.; Hossain, M.; Evans, A.; Pallister, I. Induced membrane technique for treating tibial defects gives mixed results. *Bone Joint J.* 2017, 99-B(5), 680-685.

18. Peng, W.; Zheng, W.; Shi, K.; Wang, W.; Shao, Y.; Zhang, D. An in vivo evaluation of PLLA/PLLA-gHA nano-composite for internal fixation of mandibular bone fractures. *Biomed Mater*. 2015, 10(6), 065007

19. Uhthoff H.K.; Poitras P.; Backman D.S. Internal plate fixation of fractures: short history and recent developments. J Orthop Sci. 2006, 11(2), 118-126.

20. Suto, T.; Obata, H.; Tobe, M.; Oku, H.; Yokoo, H.; Nakazato, Y.; Saito, S. Long-term effect of epidural injection with sustained-release lidocaine particlesin a rat model of postoperative pain. *Br J Anaesth.* 2012, 109(6), 957-967.

21. Yu, Y.H.; Hsu, Y.H.; Chou, Y.C.; Fan, C.L.; Ueng, S.W.N.; Kau, Y.C.; Liu, S,J. Sustained relief of pain from osteosynthesis surgery of rib fracture by using biodegradable lidocaine-eluting nanofibrous membranes. *Nanomedicine*. 2016, 12(7), 1785-1793

22. Ferguson, J.; Diefenbeck, M.; McNally, M. Ceramic biocomposites as biodegradable antibiotic carriers in the treatment of bone infections. *J Bone Jt Infect*. 2017, 2(1), 38-51.

23. Chou, Y.C. ; Lee, D. ; Chang, T.M.; Hsu, Y.H. ; Yu, Y.H.; Liu, S.J. ; Ueng, S.W. Development of a three-dimensional (3D) printed biodegradable cage to convert morselized corticocancellous bone chips into a structured cortical bone graft. *Int J Mol Sci*. 2016, 17(4), E595.

24. Casagrande, S.; Tiribuzi, R.; Cassetti, E.; Selmin, F.; Gervasi, G.L.; Barberini, L.; Freddolini, M.; Ricci, M.; Schoubben, A.; Cerulli, G.G.; Blasi, P. Biodegradable composite porous poly(dl-lactide-co-glycolide) scaffold supports mesenchymal stem cell differentiation and calcium phosphate deposition. *Artif Cells Nanomed Biotechnol.* 2017, 21, 1-11.

25. Kumbar, S.G.; Nukavarapu, S.P.; James, R.; Nair, L.S.; Laurencin, C.T. Electrospun poly(lactic acid-co-glycolic acid) scaffolds for skin tissue engineering. *Biomaterials.* 2008, 29(30), 4100-4107.

26. Wang, X.; Wei, F.; Luo, F.; Huang, K.; Xie, Z. Induction of granulation tissue for the secretion of growth factors and the promotion of bone defect repair. *J Orthop Surg Res*. 2015, 10, 147.

27. Christou, C.; Oliver, R.A.; Yu, Y.; Walsh, W.R. The Masquelet technique for membrane induction and the healing of ovine critical sized segmental defects. *PLoS One*. 2014, 9(12), e114122.

28. Masquelet, A.C. Induced membrane technique: pearls and pitfalls. *J Orthop Trauma*. 2017, 31 Suppl 5, S36-S38.

29. Giannoudis, P.V.; Faour, O.; Goff, T.; Kanakaris, N.; Dimitriou, R. Masquelet technique for the treatment of bone defects: Tips-tricks and future directions. *Injury*. 2011, 42(6), 591–598.

30. Mauffrey, C. ; Hake, M.E. ; Chadayammuri, V.; Masquelet, A,C. Reconstruction of long bone infections using the induced membrane technique: tips and tricks. *J Orthop Trauma*. 2016, 30(6), e188-e193.

31. Ma, C.H.; Chiu, Y.C.; Tsai, K.L.; Tu, Y.K.; Yen, C.Y.; Wu, C.H. Masquelet technique with external locking plate for recalcitrant distal tibial nonunion. *Injury*. 2017, 48(12), 2847–2852.